Available online at www.sciencedirect.com
SCIENCE DIRECT®
International Journal of Heat and Mass Transfer 48 (2005) 4726–4737
International Journal of HEAT and MASS TRANSFER
www.elsevier.com/locate/ijhmt

Bubble separation and collision on thin wires during subcooled boiling

J.F. Lu, X.F. Peng *

Laboratory of Phase-change and Interfacial Transport Phenomena, Department of Thermal Engineering, Tsinghua University, Beijing 100084, China

Received 21 November 2004; received in revised form 25 May 2005
Available online 10 August 2005

Abstract

An experimental investigation was conducted to observe bubble separation and collision phenomena during subcooled boiling of water on heating wires, and a theoretical model was proposed to describe the associated dynamical phenomena and understand the physical significance. Both experimental and theoretical evidences indicate that interfacial thermocapillary force induced by temperature difference and their interaction between neighbor bubbles was the most important forces during bubble separation and collision. The bubble separation process with positive effectual viscosity can be divided into two stages, accelerating and decelerating stage. The collision with an immobile bubble was concluded as an elastic collision, and the two equivalent bubbles just exchanged their momentum during their collision. Bubbles coalescence characteristics were also analyzed using the collision dynamics. The theoretical conclusions were compared with experimental results, showing a reasonable agreement with each other.

Keywords: Bubble separation; Bubble collision; Thermocapillary effect; Bubble dynamics

1. Introduction

In classical boiling investigations, dynamical and transport phenomena of a single bubble were investigated comprehensively, such as nucleation, bubble growth and departure, and associated heat transfer enhancement [1,2]. In last two decades, researchers shifted their attention to complex boiling phenomena, such as the non-linear interaction, micro phenomena and processes in a boiling system. Kenning [3,4] investigated the mutual influence and interaction between nucleation sites and bubbles by measuring wall temperature patterns. Shoji [5,6] conducted a series of investigations on the interaction of nucleation sites on the artificial surface in pool boiling and recognized the non-linear bubble dynamic characteristics. Under microgravity and/or microscale conditions, the bubble behavior and interaction was found to play an important role in boiling system [7–10].

Wang et al. [11,12] conducted a sequence of experimental investigations of subcooled boiling on extremely small Pt wires and observed complex phenomena, such as bubble sweeping and jet flows. They drew a general description that the bubble sweeping was affected by the bubble interaction and mainly driven by Marangoni effect. Sides and Tobias [13] discovered an aggregation mechanism of gas bubbles that they termed as "specific radial coalescence." In their experiments, large bubbles

* Corresponding author. Tel./fax: +86 10 6278 9751.
E-mail address: pxf-dte@mail.tsinghua.edu.cn (X.F. Peng).

0017-9310/$ - see front matter © 2005 Elsevier Ltd. All rights reserved.
doi:10.1016/j.ijheatmasstransfer.2005.05.033

Nomenclature

a	acceleration (m s^{-2})	R	radius (m)
λ	heat transfer coefficient (W m^{-1} K^{-1})	b	bubble
B	temperature coefficient of surface tension (J m^{-2} K^{-1})	t	time (s)
		c	transition state
σ	interface tension (J m^{-2})	T	temperature (K)
D	temperature gradient (K m^{-1})	i	interface
ρ	density (kg m^{-3})	u	velocity (m s^{-1})
f	force (N)	l	liquid
μ	effectual viscosity (kg m^{-1} s^{-1})	m	maximum velocity
l	distance (m)	w	wire
q	heat generation (W)	g	gas
Subscripts		*Greek symbol*	
q'	linear heat generation (W m^{-1})	α	dimensionless coefficient (–)
0	initial or reference state		

appeared to attract smaller "tracer" bubbles. Kasumi et al. [14] suggested that thermocapillary flow around neighboring bubbles on a hot wall pulled the bubbles together by establishing a perpendicular temperature gradient, and the velocity is very small.

This paper mainly presents experimental observations and associated theoretical analyses of bubble separation and collision phenomena during subcooled boiling on very thin heating wires. In the experiments, bubble separation and collision were visually observed at moderate heat fluxes. The experiments demonstrated that the associated bubble dynamical processes were partially driven by thermocapillary effect, and ideal models were proposed to investigate the characteristics of the separation and collision phenomena.

2. Experimental observation

2.1. Experiment facility

The experimental facility employed in this investigation mainly included three parts, the test section, power supply and acquisition system, as shown in Fig. 1. The testing vessel with glass window was square 250 × 250 mm and height 400 mm, which was made of stainless steel. Two copper electrodes of diameter 5 mm were led through the cover and a wire heater of platinum was horizontally installed in the vessel, and the ends of the wire were connected to two electrodes, respectively. The heated wires were about 80–100 mm long, and their diameter 100 μm. To keep liquid temperature approximately invariable at a certain temperature, the preheater and cooler was supplied, see Fig. 1. The pressure in the vessel was kept at atmospheric pressure in these experiments. The experiments employed pure water.

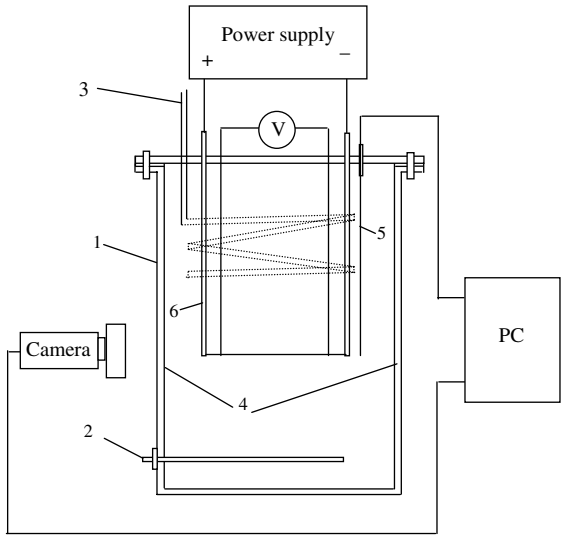

Fig. 1. Schematics of testing system: (1) testing vessel, (2) preheater, (3) cooler, (4) thermocouple, and (5) electrodes.

The power was supplied using a HP Agilent Model-6031A system, which can provide a maximum voltage of 20V and maximum power of 1000W. Direct current was applied to the wire and a uniform heat flux was generated to heat the liquid. The power supply can display the whole voltage and current. To reduce the boundary effect of the electrodes, the voltage of the investigating section was measured directly by the voltage gauge as shown in Fig. 1.

The acquisition system included photo image acquisition and data acquisition system. The photographic system included a high-speed CCD camera, a high-resolution image acquisition card, and zoom lenses. The high-speed CCD camera was a high-speed digital

imaging system (the Motionscope PCI, Redlake imaging) with a capability of up to 2000 frames. The present experiments used recording rates of 500 fps, while the resolution was 320×280 pixels. The images were sent to a computer for further analysis.

The bulk liquid temperature was measured by T-type thermocouple placed in the bulk liquid as shown in Fig. 1, and the uncertainty of the thermocouple was less than 0.2 K. The current and voltage of these investigations were measured to determine applied heat flux, and the average wire temperature was then estimated from the wire resistance by the calibrated correlation. The resistance of the wire was approximately a linear function of the temperature and the temperature coefficient of resistance, so the temperature change in resistance was then recorded during a test run that was deduced from the calibration curve. An error analysis showed the overall uncertainty of the wire temperature measurement was ± 2 K, while the uncertainty of the heat flux was less than 1%. For complex bubble motions in boiling system, their dynamic characters were mainly determined by the local temperature and other conditions but not the average temperature.

2.2. Bubble separation and collision phenomena

For subcooled liquid boiling on thin wires, stable large bubble, moving bubble and small bubble jet were normally observed. The moving bubble phenomena, such as bubble separation and collision, could usually be observed in a wide range of heat flux $0.60–1.80 \times 10^6$ W m^{-2} at liquid subcooling of 50–80 K. The detail experimental conditions of the different experimental results and observations will be presented and discussed in the followings.

Bubble separation phenomenon plays an important role during the period of initial bubble motion. A bubble separated from an immobile bubble is illustrated in Fig. 2, the water with a subcooling of 70 °C and heat flux 1.30×10^6 W m^{-2}. In the initial stage, the bubble began to separate from the left bubble. In the next 0.006 s, the bubble accelerated along the wire within the distance of about 0.25 mm, and meanwhile it grew up.

Bubble collision is another important phenomenon during subcooled boiling on thin wires. As illustrated in Fig. 3 for water with a subcooling of 70 °C and heat flux 0.6×10^6 W m^{-2}, a large bubble collided with an immobile bubble. Initially, the right bubble was at $x_0 = 0.95$ mm away from the immobile bubble and had a velocity of $u_0 \approx 40$ mm s^{-1}. After about 0.024 s, the right bubble decelerated its velocity to zero as approaching to the left one. After that, it began to return and accelerate. This collision process was just like an elastic collision.

The collision of two moving bubbles is illustrated in Fig. 4 for water with a subcooling of 70 °C at heat flux

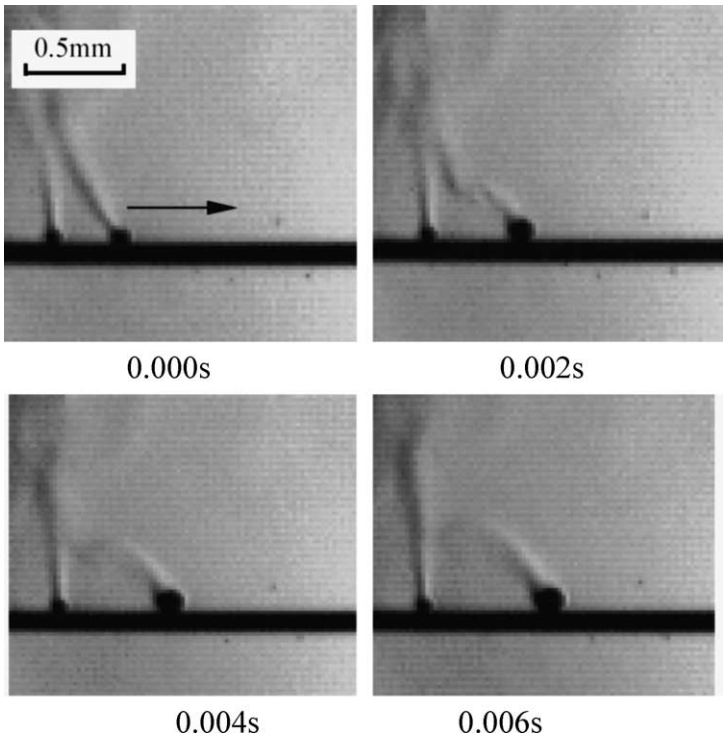

Fig. 2. Separation from an immobile bubble.

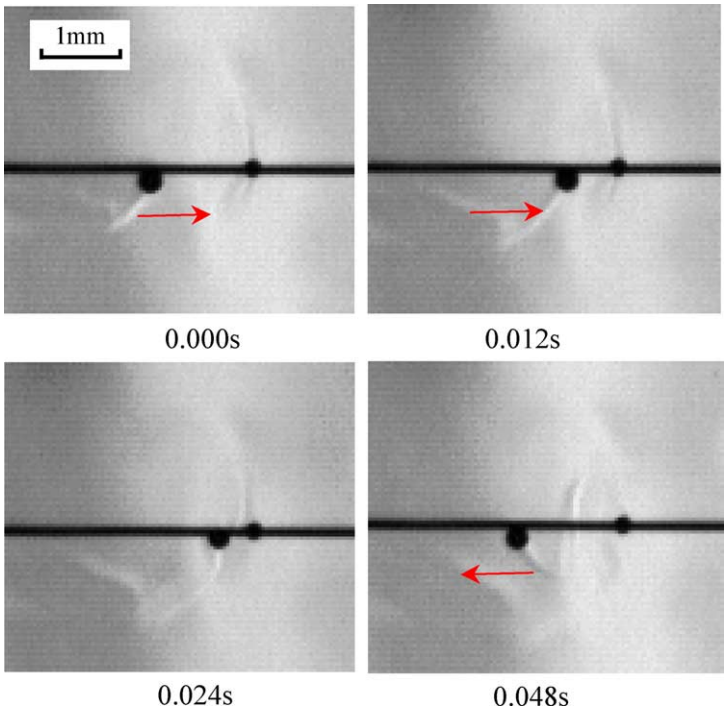

Fig. 3. Bubble collision with an immobile bubble.

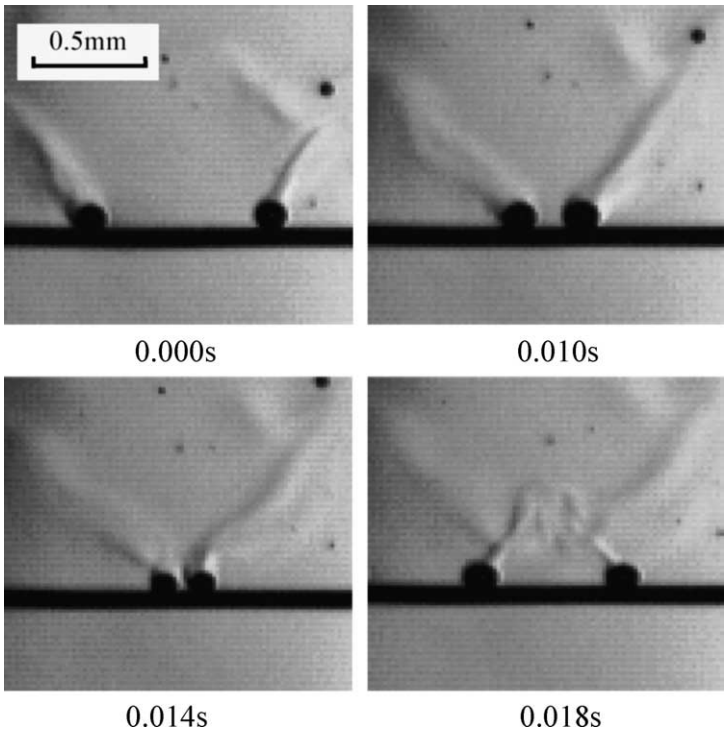

Fig. 4. Collision of two moving bubbles.

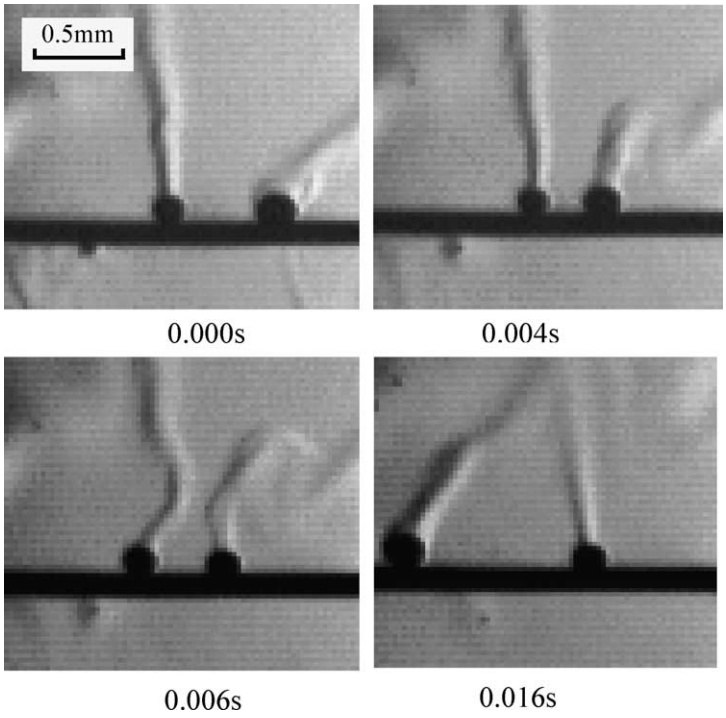

Fig. 5. Bubble movement exchange through collision.

1.6×10^6 W m^{-2}. The two bubbles initially trended to collide with each other. After colliding at about 0.014 s, they separated and moved away along two opposite directions.

Fig. 5 presents a special bubble collision process for water with a subcooling of 70 °C at heat flux of 1.30×10^6 W m^{-2}. At the beginning, the right bubble trended to collide with the left bubble. At 0.004 s, the distance of these two bubbles reached the minimum value, and the right bubble stood on the wire. A little bit later, the left bubble began to separate from the right bubble because of the interaction of these two bubbles. That is to say, the movement of the bubbles was exchanged through this interaction or collision without direct contact.

Bubble coalescence was very common observed in the experiments. Fig. 6 presents a bubble coalescence process through bubble collision for water with a subcooling of 60 °C at heat flux 0.8×10^6 W m^{-2}. Within 0.002–0.004 s, the two bubbles finished colliding and formed a larger bubble. As this larger bubble slipped to the right side, another collision occurred within time period of 0.066–0.068 s, and the right small bubble merged to the left big bubble. This type of collision made bubble growth much faster.

Apparently, the bubble motions can cause additional flow of the liquid around the bubbles and wire, and further enhance the interaction between the bubbles on the wire. These phenomena would certainly improve the heat transfer performance.

3. Bubble separation dynamics

3.1. Separation from an immobile bubble

A bubble separation is just a basic process and initial phenomenon for complex bubble dynamics. From Appendix A, the dynamical equation of a moving bubble having radius R on the wire is

$$\frac{2}{3}\pi\rho_l R^3 a = -6\pi\mu R u + \frac{8}{3}\pi\alpha D B R^2 \tag{1a}$$

$$\text{or} \quad a = -ku + c \tag{1b}$$

where $k = \frac{9\mu}{\rho_l R^2}$ is relative viscosity, $c = \frac{4\alpha B D}{\rho_l R}$ acceleration caused by thermocapillary force, α, a non-dimension coefficient, D temperature gradient in the liquid.

In a practical boiling system, the temperature distribution is very complex, and the heat transfer process includes conduction, single phase convection and phase change. For a moving bubble, the wire serves as a linear source, while the neighbor bubbles will act as cold sources and affect the horizontal temperature gradient along x. For the moving bubble in Fig. 2, the temperature gradient in the liquid is just induced by the line heater and the immobile bubble that is treated

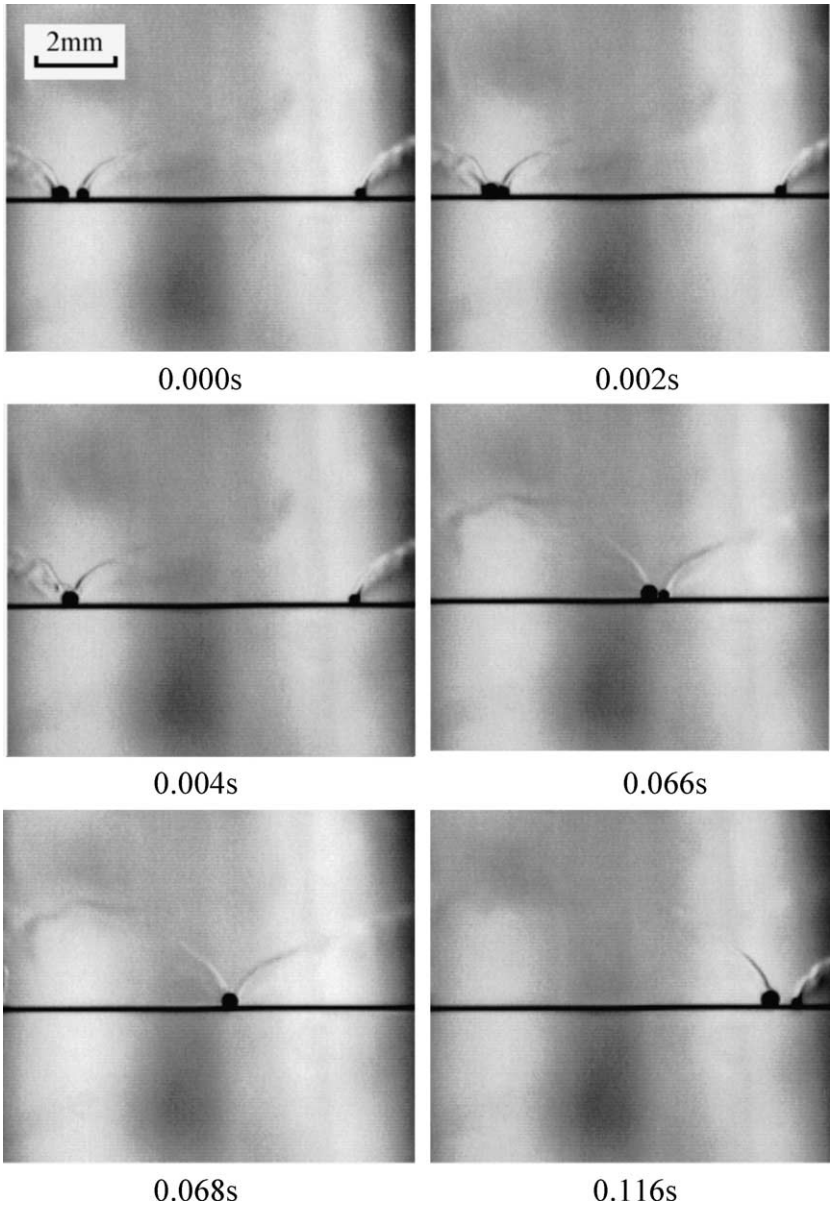

Fig. 6. Bubbles coalesce.

as a point heat source with constant surface heat flux. Since the perpendicular temperature gradient has little effect on the horizontal motion [14], only horizontal temperature gradient will be considered in this investigation. Set up a coordinate system on the wire and the origin locates at the contact point of the immobile bubble on the wire, as shown in Fig. 7.

In present investigation, the heat transfer coefficient from the around liquid and wire to the bubbles is described by a characteristic coefficient λ, which includes conductivity and convection. Since the temperature field in the surrounding liquid is only dependent upon a line source and a point sink (the static bubble), the steady temperature field can be derived as

$$T(x,y) = \frac{q_1'}{2\pi\lambda}\ln r - \frac{q_2}{4\pi\lambda\overline{OP}} + C_0 \tag{2}$$

where q_1' denotes the heat generation per unit length of the line heater, q_2 heat generation of the immobile bubble, and coefficient C_0 determined by boundary conditions. Since the temperature distribution for $x > 0$ and $x < 0$ is symmetry, and only the distribution $x > 0$ will be discussed herein.

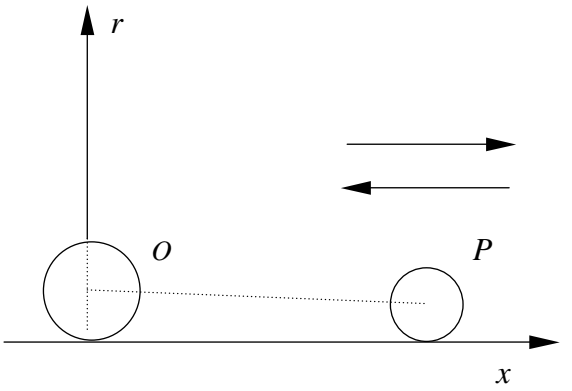

Fig. 7. Analytical model for bubble separation or collision with an immobile bubble.

For a moving bubble in Fig. 7, an arbitrary point P on the bubble is very close to the wire, and OP has a small angle with the wire, then $\overline{OP} \approx x$, and the temperature in the liquid can be expressed as

$$T = -\frac{q_2}{4\pi\lambda x} + c \quad x > 0 \tag{3}$$

where $c = \frac{q_1'}{2\pi\lambda}\ln(r_w + r_b) + c_0$, and r_w, r_b are the radius of the wire and immobile bubble, respectively. For bubble movement along horizontal direction, only the temperature profile along x is important. The external temperature gradient along x is

$$D = \frac{\partial T}{\partial x} = \frac{q_2}{4\pi\lambda x^2} \quad x > 0 \tag{4}$$

The temperature and its gradient evaluated from Eq. (3) and (4) are illustrated in Fig. 8, where dimensionless parameters $T_R = \frac{4\pi\lambda R}{q_2}(T - c)$, $D_R = \frac{4\pi\lambda R^2}{q_2}D$, $X = \frac{x}{R}$. Since the bubble acts as a cold source, the temperature along horizontal direction increases away from the bubble interface. In addition, the temperature gradient decreases quickly as the bubble separating away from immobile bubbles, mainly exhibiting two main regions. For the near bubble region or $X < 4$, the temperature gradient decreases quickly and cause significant bubble velocity variation. For the region away from bubble or $X > 4$, the temperature gradient decreases slowly and the bubble slippage becomes stable.

For bubble separation, the dynamical equation was derived as

$$a = -ku + c \tag{5a}$$

$$u(0) = 0, \quad \text{and} \quad x(0) = x_0 \tag{5b}$$

With different effectual viscosities, the separation behavior is different. For $\mu < 0$, the separating bubble will accelerate quickly during the whole process and then become unstable. For $\mu \approx 0$, substituting Eq. (4) into Eq. (5) yields

$$a = \frac{d^2x}{dt^2} = \frac{4B}{\rho_l R}\frac{\alpha q_2}{4\pi\lambda x^2} \tag{6}$$

Integrating Eq. (6) yields

$$u^2 = \frac{8B}{\rho_l R}\frac{\alpha q_2}{4\pi\lambda}\left(\frac{1}{x_0} - \frac{1}{x}\right) \tag{7}$$

where x_0 denotes bubble initial location. The bubble accelerates fast at initial time, and then it approaches to the limit velocity $u_m = \left(\frac{8B}{\rho_l R}\frac{\alpha q_2}{4\pi\lambda}\frac{1}{x_0}\right)^{1/2}$ as $x \to \infty$. From Eq. (7), the separating velocity is greatly dependent upon the intensity of the heat source q_2.

In a practical system, a bubble sometimes grows or shrinks during separation or collision, and that makes its dynamics more complex. In Fig. 2, the separating bubble significantly grew up, so it was not suit for constant radius condition. In Fig. 5, the left bubble was also a separating bubble from an immobile bubble after 0.004 s, and its volume varied not so significant. Corresponding to the experimental observation in Fig. 5, $\rho_l \approx 1000\ \mathrm{kg\,m^{-3}}$, $B = 1.7\times\ 10^{-4}\ \mathrm{Nm^{-1}\,K^{-1}}$, $R = 0.073$ mm, $x_0 = 0.37$ mm, as illustrated in Fig. 9,

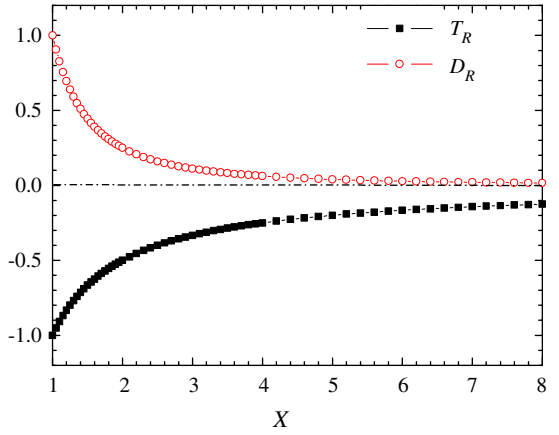

Fig. 8. Temperature and its gradient along x.

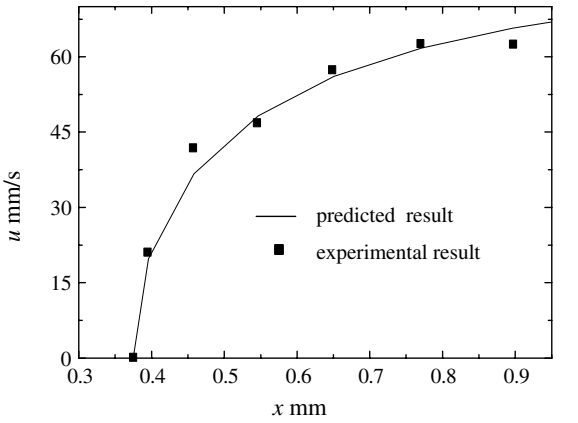

Fig. 9. Comparison of the experimental results with prediction.

the predicted results from Eq. (7) with $\frac{\alpha q_2}{4\pi\lambda} = 1.42\times 10^{-4}$ K m are compared with the experimental results, showing a good agreement with each other.

The bubble separation with $\mu > 0$ has two main stages, accelerating and decelerating process. During accelerating process, the thermocapillary force controls the motion. Since the thermocapillary force quickly decreases as increasing distance, the effectual viscosity caused by bubble motion will play a leading role after enough long time or distance moved away, and then the bubble would start the decelerating process. These two stages can be idealized as pure thermocapillary and effectual viscosity control processes.

In the thermocapillary control process, the separating dynamics is just described as Eqs. (6) and (7) by ignoring the effectual viscosity. The transition from acceleration to deceleration appears when the thermocapillary force is equal to the viscous force. Let Eq. (5) equal to zero, and the transition position is obtained as

$$\frac{9\mu}{\rho_1 R^2}u = \frac{4B}{\rho_1 R}\cdot\frac{\alpha q_2}{4\pi\lambda x_c^2} \tag{8}$$

Since the transition velocity is approximate to the limit velocity u_m, the transition point is derived as

$$x_c = \left(\frac{4\alpha BR}{9\mu u_m}\cdot\frac{q_2}{4\pi\lambda}\right)^{1/2} \tag{9}$$

During decelerating process, the thermocapillary force is ignored, and Eq. (5) evolves to

$$a = -ku \tag{10a}$$

$$u(t_c) \approx u_m \quad \text{and} \quad x(t_c) \approx x_c \tag{10b}$$

and bubble velocity is

$$u(t) = u_m \exp[-k(t - t_c)] \tag{11}$$

The moving distance after the transition is

$$l(t) = \int_{t_c}^{t} u\,dt = u_m[1 - \exp(-k(t - t_c))]/k \tag{12}$$

where $l = x - x_c$. As $t \to \infty$, $l_\infty = u_m/k$, and the velocity after the transition is

$$u(l) = u_m - kl = u_m - k(x - x_c) \tag{13}$$

Corresponding to a separating case with positive effectual viscosity in the experiments, for example, $R = 0.3$ mm, $\mu \approx 4.6\times 10^{-6}$ Ns m^{-1}, $x_0 = 1.0$ mm and $\frac{\alpha}{4\pi\lambda}q_2 = 9\times 10^{-5}$ K m. From the two-stage model, the maximum velocity $u_m \approx 20.4$ mm s^{-1}, the transition position $x_c = 4.66$ mm, and the separating velocity changing with the distance is shown as line 1 in Fig. 10. By considering both thermocapillary and effectual viscous force during the whole process, the separating velocity calculated from Eq. (5) is as line 2 in Fig. 10. The associated change of distance and velocity with time is illustrated in Fig. 11. Apparently, the two-stage model is a good approximation.

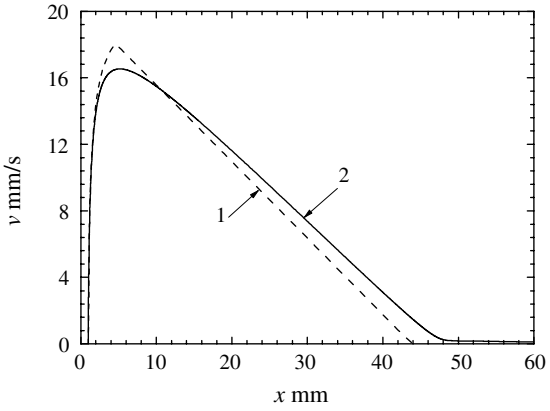

Fig. 10. Separating velocity as along x.

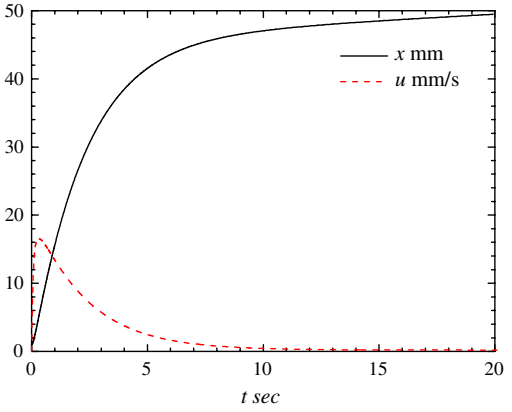

Fig. 11. Variation of separating velocity and distance with time.

3.2. Separation of two equivalent moving bubbles

For separation of two equivalent moving bubbles, having opposite moving direction, only the right bubble need to be considered because of symmetry, and the system is shown in Fig. 12. For the right moving bubble at

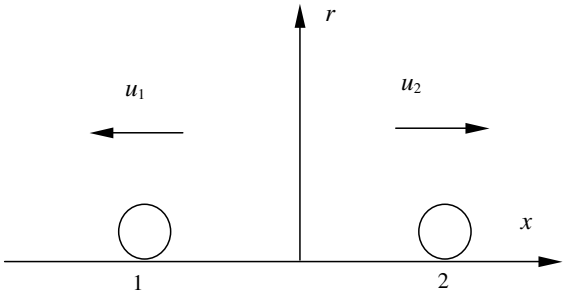

Fig. 12. Two bubble separation or collision.

x, the local temperature gradient is determined by the line heat source and point heat source at $-x$.

Similarly, the temperature gradient along x is

$$\frac{\partial T}{\partial x} = \frac{q_2}{4\pi\lambda(x+x)^2} = \frac{q_2/4}{4\pi\lambda x^2} \tag{14}$$

Ignoring effectual viscosity in the accelerating process and substituting Eq. (14) into Eq. (5) yields

$$\frac{\mathrm{d}^2x}{\mathrm{d}t^2} = \frac{1}{4}\frac{4\alpha B}{\rho_1 R}\cdot\frac{q_2}{4\pi\lambda x^2} \tag{15}$$

Accordingly, the separating velocity will be

$$u = \frac{1}{2}\left(\frac{8B}{\rho_1 R}\frac{\alpha q_2}{4\pi\lambda}\right)^{1/2}\left(\frac{1}{x_0}-\frac{1}{x}\right)^{1/2} \tag{16}$$

This velocity is just a half of a single bubble separation velocity in the accelerating region.

3.3. Separation of two non-equivalent bubbles

In usual cases, two moving bubbles have radius of r_{b1} and r_{b2} locate at $-x_1$ and x_2 with $u_{01} = u_{02} = 0$ respectively, similar to Fig. 12. Ignoring the effectual viscosity in the accelerating process and from Eq. (5), accelerations of two bubbles are derived as

$$a_1 = \frac{\mathrm{d}^2x_1}{\mathrm{d}t^2} = \frac{4\alpha B}{\rho_1 r_{b1}}\cdot\frac{q_{b2}}{4\pi\lambda l^2} \tag{17a}$$

$$a_2 = \frac{\mathrm{d}^2x_2}{\mathrm{d}t^2} = \frac{4\alpha B}{\rho_1 r_{b2}}\cdot\frac{q_{b1}}{4\pi\lambda l^2} \tag{17b}$$

where $l = x_1 + x_2$. Since the ratio of these two accelerations is $\frac{a_1}{a_2} = \frac{\mathrm{d}^2x_1}{\mathrm{d}t^2}\Big/\frac{\mathrm{d}^2x_2}{\mathrm{d}t^2} = \frac{r_{b2}q_{b2}}{r_{b1}q_{b1}} = \psi$, to simplify the bubble motion, select the origin to satisfy $x_{01}/x_{02} = \psi$, and then

$$x_1/x_2 = \psi \tag{18a}$$

$$l = x_1(1+\psi)/\psi = x_2(1+\psi) \tag{18b}$$

Substituting Eq. (18) into Eq. (17) yields

$$\frac{\mathrm{d}^2l}{\mathrm{d}t^2} = \frac{4\alpha B}{\rho_1}\cdot\frac{1}{4\pi\lambda l^2}\left(\frac{q_{b1}}{r_{b2}}+\frac{q_{b2}}{r_{b1}}\right) \tag{19}$$

Integrating Eq. (19), we have,

$$u_1 = \left[\frac{8\alpha B}{\rho_1}\frac{1}{4\pi\lambda}\left(\frac{q_{b1}}{r_{b2}}+\frac{q_{b2}}{r_{b1}}\right)\cdot\left(\frac{1}{l_0}-\frac{1}{l_1}\right)\right]^{1/2} \tag{20}$$

If $\psi = 1$, $u_1 = \frac{1}{2}\left[\frac{8B}{\rho_1 r_{b2}}\cdot\frac{\alpha q_{b1}}{4\pi\lambda}\left(\frac{1}{l_0/2}-\frac{1}{l/2}\right)\right]^{1/2} = \frac{1}{2}\left[\frac{8B}{\rho_1 r_{b1}}\cdot\frac{\alpha q_{b2}}{4\pi\lambda}\times\left(\frac{1}{l_0/2}-\frac{1}{l/2}\right)\right]^{1/2}$, that is consistent with Eq. (16). When $\psi \ll 1$, $u_1 = \left[\frac{8\alpha B}{\rho_1}\frac{q_{b1}}{4\pi\lambda r_{b2}}\cdot\left(\frac{1}{l_0}-\frac{1}{l_1}\right)\right]^{1/2}$, this is similar to the bubble separation away from an immobile bubble described by Eq. (7).

4. Bubble collision dynamics

4.1. Collision with an immobile bubble

For a bubble collision with an immobile bubble, as illustrated in Figs. 3–6, in a system of Fig. 7 the dynamical equation of the moving bubble is similar to separation phenomenon, or

$$\frac{2}{3}\pi\rho_1 R^3 a = -6\pi\mu R u + \frac{8}{3}\pi\alpha DBR^2 \tag{21a}$$

$$u(0) = -u_0 < 0, \quad \text{and} \quad x(0) = x_0 \tag{21b}$$

The thermocapillary force acts as a resistance when the bubble moves close to the immobile bubble, and the main difference from separation dynamics is the initial conditions. As noted, the viscosity could be ignored in a short collision length, and the dynamic equation evolves to

$$u^2 = u_0^2 - \frac{8B}{\rho_1 R}\cdot\frac{\alpha q_2}{4\pi\lambda}\left(\frac{1}{x}-\frac{1}{x_0}\right) \tag{22}$$

Apparently, a collision process can be divided into two stages, approaching to the immobile bubble for a decelerating process and separating from the bubble for an accelerating process. Setting velocity u to zero, the critical distance of these two bubbles is

$$x_c = \left[\frac{1}{x_0}+u_0^2\left(\frac{8B}{\rho_1 R}\cdot\frac{\alpha q_2}{4\pi\lambda}\right)^{-1}\right]^{-1} \tag{23}$$

As reaching to x_c the bubble turns to separation from the immobile bubble and the thermocapillary force accelerates the bubble. The whole process is illustrated in Fig. 13, where $X = x/x_0$ and $u_{00} = \left(\frac{8B}{\rho_1 R}\cdot\frac{\alpha q_2}{4\pi\lambda x_0}\right)^{1/2}$, the dimensionless distance and characteristic velocity, respectively. And $\chi = u_0/u_{00}$ denotes dimensionless initial velocity.

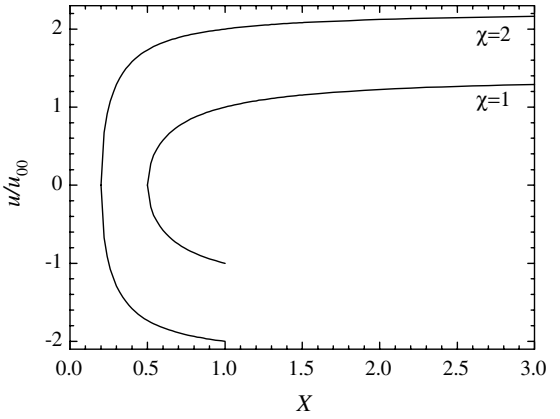

Fig. 13. Bubble collision with different initial velocities.

From Fig. 13 and Eq. (22), the collision characteristics are mainly dependent upon the dimensionless initial velocity χ. The bubble motion is almost symmetry about the critical point in the nearby zone, and the process is like an elastic collision. The dimensionless critical distance will be smaller for large χ, and the two bubbles can approach to each other much close. Also, the bubble with large χ reverses its velocity very sharply near the critical point, while the bubble with little χ reverses much smoothly.

Corresponding to the experimental observation in Fig. 3, $R = 0.15$ mm, $x_0 = 0.95$ mm s^{-1}, $u_0 = -40$ mm s^{-1}, the characteristics of the collision is discussed here. As illustrated in Fig. 14, the predicted results from Eq. (22) with $\frac{\gamma q_2}{4\pi\lambda} = 8.2 \times 10^{-5}$ K m are compared with the experimental results, showing a good agreement with each other.

4.2. Collision of two equivalent bubbles

For the collision of two equivalent moving bubbles having initial velocity u_{01} and u_{02}, respectively, the thermocapillary forces is equal and opposite. From the momentum conservation, the bubble velocities satisfy $u_1 + u_2 = u_{01} + u_{02}$ and the velocity of the centre of two bubbles is $u_0 = (u_{01} + u_{02})/2$. Setting a moving system with the origin at the center of two bubbles, similar to Fig. 12, the relative initial velocity is $u'_{01} = (u_{01} - u_{02})/2$ and $u'_{02} = (u_{02} - u_{01})/2$, and the initial coordinates are $-x'_{01}$ and x'_{01}, respectively.

Because the dynamics of the two bubbles is symmetrical in the new coordinate system, only one bubble is considered. The motion of the right moving bubble can be described by Eq. (15), and the velocity is

$$u_2'^2 = u_{02}'^2 - \frac{2B}{\rho_1} \cdot \frac{q_2}{4\pi\lambda} \left(\frac{1}{x'_2} - \frac{1}{x'_{02}} \right) \tag{24}$$

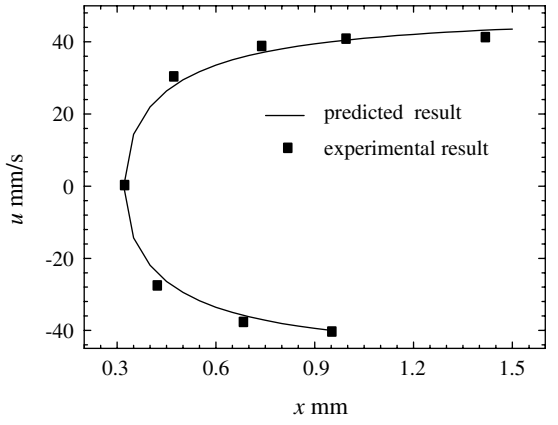

Fig. 14. Comparison of the experimental results and prediction.

When the bubble returns to $x'_2 = x'_{02}$, $u'_2 = u'_{02}$, and its velocity is

$$u_2 = u'_2 + u_0 = u_{01} \tag{25}$$

This holds true for another bubble, or $u_1 = u_{02}$. This exactly implies that the two moving bubbles just exchange their velocity after the collision as the experimental phenomenon shown in Fig. 4. However, a special collision was observed in Fig. 5, the left still bubble gaining velocity while the right bubble halting after the collision.

Similar to Eq. (23), the two bubbles have a minimum distance when the velocities of two bubbles are just as $u'_1 = u'_2 = 0$, and the minimum distance is

$$x_c = \left[\frac{1}{x'_1} + u_{01}'^2 \left(\frac{2B}{\rho_1} \cdot \frac{q_2}{4\pi\lambda} \right)^{-1} \right]^{-1} \tag{26}$$

Because of symmetry, the minimum distance between two bubbles is $l_c = 2x_c$.

As noted above, bubble collision is dependent upon relative velocity, relative distance and bubble radius. Since the thermocapillary force induced by two different bubbles is usually not equal, the system with two bubbles does not satisfy the momentum conservation, and there is no symmetry coordinate to simplify collision process. As in normal cases, initial conditions are of critical important for collision behavior.

4.3. Bubble coalescence

Usually, two bubbles would coalesce if the distance between the two bubbles is smaller than the sum of the two bubble radii. For a moving bubble colliding with an immobile bubble, the coalescing condition from Eq. (23) is

$$x_c = \left[\frac{1}{x_0} + u_0^2 \left(\frac{8\alpha B}{\rho_1 R} \cdot \frac{q_2}{4\pi\lambda} \right)^{-1} \right]^{-1} < R + r_b \tag{27}$$

When the initial distance x_0 is large enough, $\frac{q_2}{4\pi\lambda} < \frac{\rho_1 (R + r_b) R u_0^2}{8B}$. Obviously, the moving bubble will coalesce with the immobile bubble if the cold source of immobile bubble is not so large or the initial velocity is high enough. The relative velocity between two bubbles would promote the coalescence process. For two equivalent moving bubbles, the coalescing criteria from Eq. (26) is,

$$l_c = 2 \left[\frac{1}{x'_1} + \left(\frac{u_{01} - u_{02}}{2} \right)^2 \left(\frac{2B}{\rho_1} \cdot \frac{q_2}{4\pi\lambda} \right)^{-1} \right]^{-1} < 2r_b \tag{28}$$

If x'_1 is large enough, and $\frac{q_2}{4\pi\lambda} < \frac{2\rho_1 r_b (u_{01} - u_{02})^2}{B}$. Small cold source and/or higher relative velocity makes coalescing easy.

Due to bubble coalescence, the bubbles would grow and depart fast, which should enhance the boiling heat transfer.

5. Conclusions

Both experimental observation and theoretical analyses were conducted to understand bubble separation and collision during subcooled liquid boiling on very small heating wires. Bubble separation process with positive effectual viscosity can be theoretically divided into accelerating and decelerating stage. The collision with an immobile bubble is just as elastic collision, which is almost symmetrical about the critical point according to the theoretical and experimental investigation. For the collision of two equivalent bubbles, the bubbles just exchange their velocities. The intensity and initial velocity of cold sources play important roles in the bubble coalescence during bubble collision. The theoretical results were compared with experimental results and showed a reasonable agreement with each other.

Acknowledgement

This research is currently supported by Specialized Research Fund for the Doctoral Program of Higher Education (Contract no. 20040003076).

Appendix A. Derivation of bubble dynamical equation

When a bubble accelerates or decelerates on a horizontal wire, the inertial effect will play an important role in the bubble motion. For a sphere submerged in water, the equivalent inertial mass of the liquid is [15]

$$m' = \frac{1}{2}\rho_l V \tag{A.1}$$

And the inertial force of the bubble is derived as

$$ma = (m' + \rho_g V)a \approx m_a a = \frac{2}{3}\pi\rho_l R^3 a \tag{A.2}$$

When a bubble moves with an arbitrary velocity, the viscosity force will act as a resistance force, while the thermocapillary force induced by the bubble motion itself will act as a drive force [12]. If the whole effect caused by bubble motion is considered as effectual viscosity and similar to Stokes' law, it can be expressed as

$$f_v = -6\pi\mu R u \tag{A.3}$$

where μ is the effectual viscosity.

For a complex bubble dynamic system, some cold sources such as a bubble nearby or boundaries will cause the temperature difference between two sides of a bubble in the liquid, which could induce external thermocapillary force beside the forces caused by the bubble motion. Consider a bubble, as shown in Fig. 15, the drive force along x is expressed as

$$f_d = -\int_0^{\pi} \frac{\partial\sigma(T_i)}{\partial T_i}\frac{dT_i}{R\,d\theta} 2\pi R \sin\theta \sin\theta R\, d\theta \tag{A.4}$$

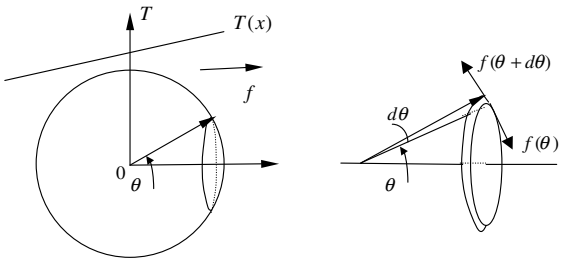

Fig. 15. Thermal drive force on a bubble.

As an initial approach for theoretical investigation, the interface temperature gradient along the bubble interface has a linear relation with the bulk temperature gradient or $dT_i(x)/dx = \alpha \cdot dT(x)/dx = \alpha D$, where $0 < \alpha < 1$, and D denotes the horizontal temperature gradient caused by cold sources. Integrating Eq. (A.4) yields

$$f_d = \frac{8}{3}\pi\alpha D B R^2 \tag{A.5}$$

where $d\sigma/dT_i = -B$ [1].

From Eqs. (A.2)–(A.4), the dynamical equation of a moving bubble on a heating wire is

$$ma = \frac{2}{3}\pi\rho_l R^3 a = -6\pi\mu R u + \frac{8}{3}\pi\alpha B R^2 \tag{A.6a}$$

$$\text{or} \quad a = -ku + c \tag{A.6b}$$

where $k = \frac{9\mu}{\rho_l R^2}$ is relative effectual viscosity $c = \frac{4\alpha B D}{\rho_l R}$ acceleration caused by the thermocapillary force. From Eq. (A.6), the bubble dynamic process is obviously controlled by the effectual viscosity force and external thermocapillary force.

References

[1] V.P. Carey, Liquid–Vapor Phase-Change Phenomena: An Introduction to the Thermophysics of Vaporization and Condensation Processes in Heat Transfer Equipment, Hemisphere Pub. Corp., New York, 1992.
[2] H.K. Forster, N. Zuber, Dynamics of vapor bubble and boiling heat transfer, AIChE J. 1 (1952) 531–535.
[3] D.B.R. Kenning, H.M. Victor, Fully-developed nucleate boiling: overlap of areas of influence and interference between bubble sites, Int. J. Heat Mass Transfer 24 (1981) 1025–1032.
[4] D.B.R. Kenning, Wall temperature patterns in nucleate boiling, Int. J. Heat Mass Transfer 35 (1992) 73–85.
[5] L. Zhang, M. Shoji, Nucleation site interaction in pool boiling on the artificial surface, Int. J. Heat Mass Transfer 46 (2003) 513–522.
[6] R. Mosdorf, M. Shoji, Chaos in nucleate boiling-nonlinear analysis and modeling, Int. J. Heat Mass Transfer 47 (2004) 1515–1524.
[7] J. Straub, Microscale boiling heat transfer under 0g and 1g conditions, Int. J. Therm. Sci. 39 (2000) 490–497.

[8] P.G. Deng, Y.K. Lee, P. Cheng, The growth and collapse of a micro-bubble under pulse heating, Int. J. Heat Mass Transfer 46 (2003) 4041–4050.
[9] J.Y. Jung, J.Y. Lee, H.C. Park, H.Y. Kwak, Bubble nucleation on micro line heaters under steady or finite pulse of voltage input, Int. J. Heat Mass Transfer 46 (2003) 3897–3907.
[10] A. Asai, T. Hara, I. Endo, One-dimensional models of bubble growth and liquid flow in bubble jet printer, Jpn. J. Appl. Phys. Jpn. J. Appl. Phys. 26 (1987) 1794–1801.
[11] H. Wang, X.F. Peng, B.X. Wang, D.J. Lee, Bubble sweeping and jet flows during nucleate boiling of subcooled liquids, Int. J. Heat Mass Transfer 46 (2003) 863–869.
[12] H. Wang, X.F. Peng, B.X. Wang, D.J. Lee, Bubble-sweeping mechanisms, Sci. Sina, Ser. E 46 (2003) 225–233.
[13] P.J. Sides, C.W. Tobias, Close view of gas evolution from the back side of transparent electrode, J. Electrochem. Soc. 132 (1985) 583–587.
[14] H. Kasumi, Y.E. Solomentsev, S.A. Guelcher, J.L. Anderson, P.J. Sides, Thermocapillary flow and aggregation of bubbles on a solid wall, J. Colloid Interf. Sci. 232 (2000) 111–120.
[15] T.E. Faber, Fluid Dynamic for Physicists, Cambridge University Press, Cambridge, 2001.